Behavioural Brain Research 438 (2023) 114171

Contents lists available at ScienceDirect

Behavioural Brain Research

journal homepage: www.elsevier.com/locate/bbr

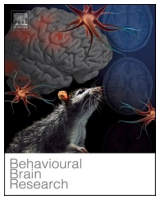

Research report

Selective orexin 1 receptor antagonist SB-334867 aggravated cognitive dysfunction in 3xTg-AD mice

Wen-Rui Gao [a], Xiao-Hong Hu [a], Kai-Yue Yu [a], Hong-Yan Cai [b], Zhao-Jun Wang [a], Lei Wang [c,*], Mei-Na Wu [a,*]

[a] Department of Physiology, Key Laboratory of Cellular Physiology, Ministry of Education, Shanxi Medical University, Taiyuan 030001, China
[b] Department of Microbiology and Immunology, Shanxi Medical University, Taiyuan 030001, China
[c] Department of Geriatrics, Third Hospital of Shanxi Medical University, Shanxi Bethune Hospital, Shanxi Academy of Medical Sciences, Taiyuan 030032, China

ARTICLE INFO

Keywords:
Alzheimer's disease (AD)
Orexin 1 receptor (OX1R)
Cognition
Synaptic plasticity
Amyloid β protein (Aβ)
Phospho-tau (p-tau)

ABSTRACT

Cognitive dysfunction is the main clinical manifestation of Alzheimer's disease (AD). Previous research found that elevated orexin level in the cerebrospinal fluid was closely related to the course of AD, and orexin-A treatment could increase amyloid β protein (Aβ) deposition and aggravate spatial memory impairment in APP/PS1 mice. Furthermore, recent research found that dual orexin receptor (OXR) antagonist might affect Aβ level and cognitive dysfunction in AD, but the effects of OX1R or OX2R alone is unreported until now. Considering that OX1R is highly expressed in the hippocampus and plays important roles in learning and memory, the effects of OX1R in AD cognitive dysfunction and its possible mechanism should be investigated. In the present study, selective OX1R antagonist SB-334867 was used to block OX1R. Then, different behavioral tests were performed to observe the effects of OX1R blockade on cognitive function of 3xTg-AD mice exhibited both Aβ and tau pathology, *in vivo* electrophysiological recording and western blot were used to investigate the potential mechanism. The results showed that chronic OX1R blockade aggravated the impairments of short-term working memory, long-term spatial memory and synaptic plasticity in 9-month-old female 3xTg-AD mice, increased levels of soluble Aβ oligomers and p-tau, and decreased PSD-95 expression in the hippocampus of 3xTg-AD mice. These results indicate that the detrimental effects of SB-334867 on cognitive behaviors in 3xTg-AD mice are closely related to the decrease of PSD-95 and depression of *in vivo* long-term potentiation (LTP) caused by increased Aβ oligomers and p-tau.

1. Introduction

Cognitive dysfunction is the main clinical manifestation of Alzheimer's disease (AD), a neurodegenerative disease account for more than two-thirds of dementia in the world [1]. The characterized pathological features of AD are senile plaques mainly composed of β amyloid protein (Aβ) and neurofibrillary tangles formed by abnormal phosphorylation of tau protein. According to previous reports, Aβ oligomers played an important neurotoxic role in the course of AD [2], abnormal hyperphosphorylated tau protein caused synaptic loss, damage to axonal transport and cytoskeletal dysfunction [3]. More importantly, the two pathologies have synergistic effects [4]. Although Aβ may initiate the cascade of events, tau impairment is likely the effector molecule of neurodegeneration [5], which indicated the importance of using animal model exhibited both Aβ and tau pathology.

Orexins/hypocretins are neuropeptides synthesized by neurons in the lateral hypothalamus, which play important roles in regulating sleep-wake cycle, mood and cognition [6]. Recent studies found that orexin level in the cerebrospinal fluid (CSF) was closely related to the course of AD. In patients with mild cognitive impairment (MCI), abnormally elevated orexin-A in the CSF was observed, along with lower Aβ1–42 level, higher total tau (t-tau) and phosphorylated tau (p-tau) levels [7]. In AD patients, increase of orexin-A, and abnormal levels of p-tau and Aβ1–42 were observed in the CSF, accompanied with significant decrease in the mini-mental state examination (MMSE) score [8–11]. In animal models, recent research observed higher density and distribution of orexin A-positive neurons in the brain of APP/PS1 mice [12]; orexin-A treatment increased Aβ deposition in the brain of APP/PS1 mice and aggravated spatial memory deficits in the Morris water maze test [13].

* Corresponding authors.
E-mail addresses: wang_leicn2021@163.com (L. Wang), wmna@163.com (M.-N. Wu).

https://doi.org/10.1016/j.bbr.2022.114171
Received 18 July 2022; Received in revised form 9 October 2022; Accepted 20 October 2022
Available online 21 October 2022

There are two types of orexin receptors, orexin 1 receptor (OX1R) and orexin 2 receptor (OX2R). OX1R is highly expressed in the hippocampus [14] and is important to learning and memory regulation [15,16]. Some research found that knockdown of OX1R in the hippocampal CA1 region by injection of adeno-associated virus could lead to impaired spatial memory and decreased density of apical dendritic spines in CA1 region in rats [17]. OX2R is also expressed in the hippocampus, but up-regulation of OX2R in the hippocampus and impairment of spatial memory were observed in single prolonged stress rats [18]. Recently, there are a few reports about effects of dual orexin receptor antagonist (DORA) on Aβ level and cognitive dysfunction in AD, but the results from different studies are inconsistent. Kang et al. found that chronic intracerebroventricular (i.c.v.) injection of almorexant could significantly reduce Aβ plaques in the cortex of APP/PS1 mice [19]; our previous research also found that chronic oral administration of suvorexant could reduce Aβ deposition in the brain of APP/PS1 mice and improve its learning and memory impairments [20]. However, chronic administration of DORA-22 did not affect short-term working memory and the density of Aβ plaques in 5xFAD mice mainly exhibited Aβ pathology [21]. Considering that the use of DORA could not confirm which subtype of OXR plays a major role in AD pathogenesis, and there is lack of research about effects of OX1R or OX2R alone in AD, it is important to further investigate the effects of OX1R or OX2R alone in AD.

Because OX1R is highly expressed in the hippocampus and exert important roles in cognitive function, the effects and potential mechanism of OX1R on cognitive dysfunction in AD was investigated in the present study. Firstly, the effects of OX1R on cognitive dysfunction in 3xTg-AD mice exhibited both Aβ deposition and abnormal tau phosphorylation [22] were observed by using multiple behavioral tests, then the possible electrophysiological and molecular mechanism were investigated by using *in vivo* electrophysiological recording and western blot, which could provide experimental evidence for further clarifying the role and mechanism of OX1R in the course of AD.

2. Materials and methods

2.1. Animals and treatment

Considering that females are at higher risk of developing AD compared with males [23], and the pathological phenotype of female 3xTg-AD mice is more obvious than that of males [24,25], 9-month-old female 3xTg-AD mice (Jackson Laboratory, USA) and non-transgenic wild-type (WT) mice were used. All procedures were performed in accordance with the guidelines established by the ethics committee for the use of experimental animals at Shanxi Medical University. All mice were housed in the SPF laboratory animal room of Shanxi Medical University under a 12 h/12 h light-dark cycle, and received standard rodent food and water ad libitum. The 3xTg-AD mice and WT mice were randomly divided into four groups: WT+Vehicle, WT+SB-334867, 3xTg-AD+Vehicle and 3xTg-AD+SB-334867 (n = 10 for each group). SB-334867 (20 mg/kg, InvivoChem, USA) or equal volume of 10% hydroxypropyl-β-cyclodextrin (Vehicle) solution was intraperitoneal injected once a day [26] before turning off the lights at 18:00. After 28 days of continuous administration, different behavioral tests were performed in sequence. All behavioral experiments were carried out during the activity period of mice under dim red light (<10 Lx) [27], and the drug was administered continuously during the behavioral experiments.

2.2. Object recognition test

The experiment was consisted of acquisition phase and testing phase. In the acquisition phase, two identical objects were placed symmetrically in the object recognition experimental box, and the mouse was allowed to explore freely for 10 min. The testing phase was performed 6 h later. A novel object was put into the experimental box, and the mouse was allowed to freely explore for another 10 min. The exploration time of familiar object and novel object was recorded, and the recognition index (RI) and discrimination index (DI) of mice were calculated. RI = time to explore novel object / (time to explore old object + time to explore novel object) × 100%, DI = (time to explore novel object - time to explore novel object) / (time to explore old object + time to explore novel object) × 100% [28]. This test assumes that a mouse not recognizing the object have a random chance of exploring each object (50%). A mouse which identifies one of the objects as new will spend more time exploring it. Therefore, its RI will be higher than 50%, and a lack of discrimination between the novel and the familiar object, *i.e.*, a RI of 50% or below, was interpreted as impaired object recognition [29].

2.3. Y-maze spontaneous alternation test

The Y-maze consists of three closed arms with equal length (30 cm long × 12 cm high × 5 cm wide) connected at angles of 120°. Each mouse was placed in the triangle area in the middle of the Y-maze and allowed to explore freely for 8 min. The total number of entering the arm and the order of exploration of the arms were recorded. The percentage of correct spontaneous alteration was calculated as [(number of correct alternations) / (total number of arm entries −2)] × 100% [30].

2.4. Morris water maze test

The experiment included three parts: the hidden platform test, the probe test and the visible platform test [31]. The maze is a circular pool with a diameter of 120 cm and height of 50 cm. Four markers with different shapes are isometrically affixed to the white inner wall as visual references for mice. Before the beginning of experiment, tap water was poured into the maze and temperature was controlled at 22 ± 2 ℃. The maze was divided into four quadrants by software (Smart 3.0, Panlab Harward Apparatus, USA), and an escape platform 1 cm below the water surface was placed in the target quadrant. In the hidden platform test, each mouse was put into the water from the midpoint of the four quadrants to swim for 60 s, and the escape latency was recorded. Each mouse was trained four times per day for 5 consecutive days. In the probe test on the 6th day, the underwater escape platform was removed, and each mouse was put into the water from the same position of any two quadrants except the target quadrant. The swimming track of each mouse was recorded, then the number crossed the platform and the percentage of swimming time in the target quadrant of mice were calculated. In the visible platform test, the escape platform 1 cm above the water surface was placed in any quadrant except the target quadrant, and the time of mice to reach the platform was recorded. In addition, the swimming speed of mice in each group at three experimental phases was recorded.

2.5. In vivo hippocampal electrophysiological recording

In vivo hippocampal field potential recordings were performed after the cognitive behavioral experiments. Each mouse was anesthetized by intraperitoneal injection of 5% chloral hydrate (7 ml/kg), and then fixed in the brain stereotaxic apparatus (68016, RWD Life Science, China). The skull was exposed, holes were drilled and the dura was removed. The tips of the stimulating and recording electrodes were located at the Schaffer collateral/commissural pathway and the stratum radiatum of the hippocampal CA1 region, respectively. As described previously [32], the field excitatory postsynaptic potentials (fEPSPs) were evoked with gradually increased stimuli (0–0.2 mA with 0.02 mA increments; duration: 50 μs) at a frequency of 0.033 Hz, and the input-output curve (I-O curve) was drawn firstly. Then, baseline fEPSPs were evoked by test stimulus (intensity: 30%−50% of the maximum stimulus, frequency: 0.033 Hz) and recorded for 30 min, paired-pulse facilitation (PPF) generally agreed to be of presynaptic origin and reflected the probability of transmitter release [33] was initiated by paired stimuli with an interval of 50 ms. Finally, high frequency stimulation (HFS, 3 trains of 20

stimuli at 200 Hz with an inter-train interval of 30 s) was given to induce long-term potentiation (LTP), and the recording of fEPSPs was continued for at least 60 min with the same intensity of basal fEPSPs.

2.6. Western blot

After the *in vivo* electrophysiological recording, mice randomly selected from each group were anesthetized, and hippocampal tissue was quickly removed on ice. According to the net weight of mouse hippocampus tissue, RIPA lysate (10 ml/g), PMSF (1:100) and broad-spectrum phosphatase inhibitor (1:100) were added in turn and the protein was extracted (Tissue Protein Extraction Reagent, Boster, China). The fully lysed tissue was centrifuged at 13,000 r/min for 25 min, and the supernatant was extracted to measure the protein concentration with BCA protein quantification kit (AR0146, Boster, China). Then, the proteins were separated by electrophoresis, samples were transferred to polyvinylidene difluoride membrane. After blocking nonspecific binding by 5% bovine serum albumin, the samples were incubated with primary antibodies post-synaptic density 95 (PSD-95, 1:1000, ab76115, Abcam, UK), synaptophysin (SYP, 1:1000, mAb#36406, Cell Signaling Technology, USA), 6E10 (1:10000, 803015, Biolegend, USA), PhosphoT231 (1:5000, ab151559, Abcam, UK), tau (1:5000, ab76128, Abcam, UK), OX1R (1:1000, AB3092, Sigma-Aldrich, USA), OX2R (1:1000, ab183072, Abcam, UK), β-tubulin (1:5000, AP0064, Bioworld Technology, USA) and GAPDH (1:5000, AP0063, Bioworld Technology, USA) overnight at 4°C, and detected with secondary antibody (goat anti-rabbit IgG-HRP conjugate, 1:5000, BA1054, Boster, China; goat anti-mice IgG-HRP conjugate, BA1050, Boster, China). The bands were detected with BeyoECL Plus kit (P0018M, Beyotime, China), scanned with detection system (FluorChem FC3, ProteinSimple, USA) and analyzed by Image J analysis software.

2.7. Statistical analysis

Statistical analysis was using SPSS 18.0 and Sigmaplot 14.0. All results were presented as mean ± standard error of the mean (SEM). Three-way repeated measures analysis of variance (ANOVA) was used to analyze the escape latency in the MWM test. Two-way ANOVA and 2-sample t-test were used for western blot analysis, other data were analyzed using two-way ANOVA and *post hoc* Tukey's multiple comparison tests. $P < 0.05$ was considered statistically significant.

3. Results

3.1. SB-334867 aggravated the impairment of short-term working memory in 3xTg-AD mice

In the object recognition test, the object recognition index (RI, Fig. 1A) and discrimination index (DI, Fig. 1B) in WT+Vehicle group were 59.1% ± 4.8% and 18.3% ± 9.7%, respectively. Compared with WT+Vehicle group, the RI and DI in 3xTg-AD+Vehicle group significantly decreased to 38.1% ± 4.2% ($P = 0.003$) and − 23.3% ± 8.4% ($P = 0.002$), indicating that APP/PS1/tau gene mutation impaired object recognition of mice. At the same time, both RI ($P = 0.008$) and DI ($P = 0.006$) of WT mice were significantly decreased after SB-334867 treatment, indicating that OX1R antagonist SB-334867 impaired object recognition memory in WT mice. In addition, SB-334867 treatment further decreased the RI ($P = 0.015$) and DI ($P = 0.042$) in 3xTg-AD mice. (2-way ANOVA: RI: genotype: $F_{(1,39)} = 18.391$, $P < 0.001$; treatment: $F_{(1,39)} = 14.553$, $P < 0.001$; genotype x treatment: $F_{(1,39)} = 0.039$,

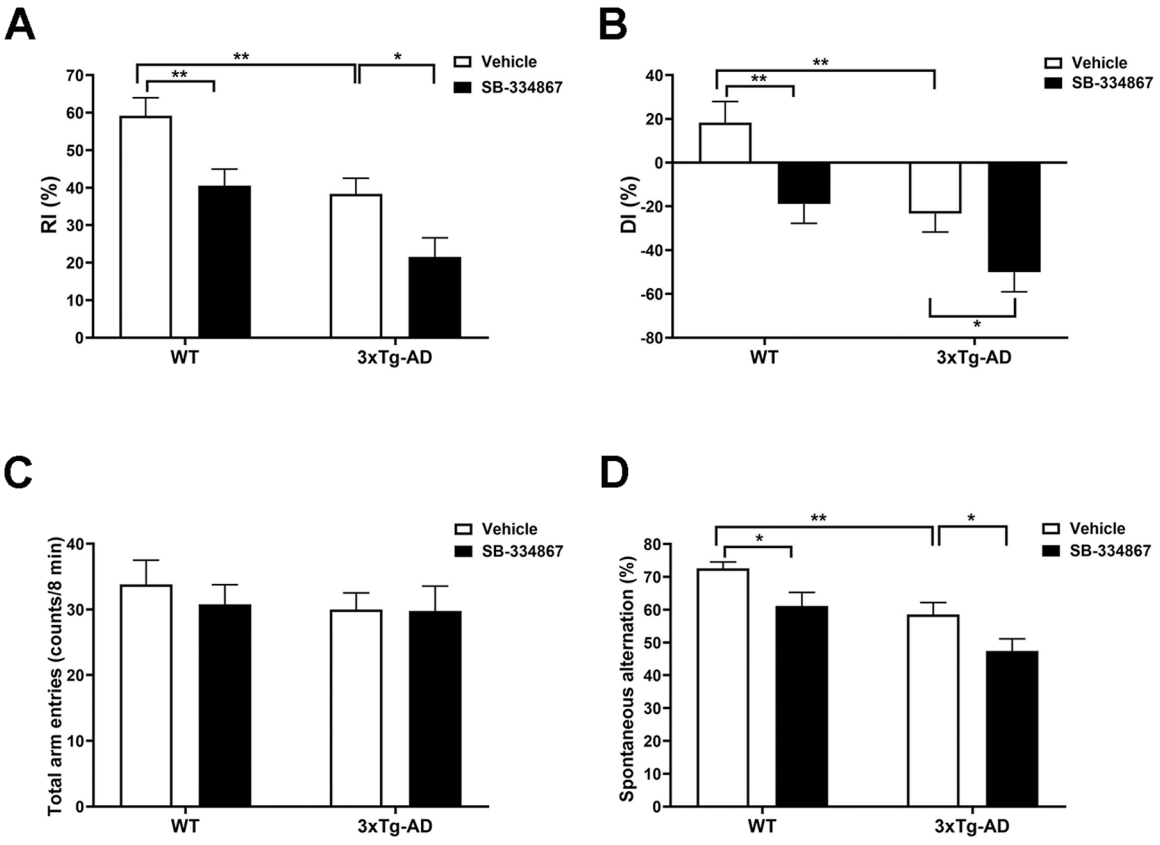

Fig. 1. SB-334867 aggravated the impairment of short-term working memory in 3xTg-AD mice. (A - B) Bar graphs showing the decreased recognition index (RI) and discrimination index (DI) of 3xTg-AD mice and WT mice after SB-334867 treatment. (C) Bar graphs showing no significant difference in the total number of arm entries among the four groups. (D) Bar graphs showing the decreased correct spontaneous alternation of 3xTg-AD mice and WT mice after SB-334867 treatment (n = 10, * $P < 0.05$, ** $P < 0.01$).

$P = 0.845$. DI: genotype: $F_{(1,39)} = 16.505$, $P < 0.001$; treatment: $F_{(1,39)} = 12.759$, $P = 0.001$; genotype x treatment: $F_{(1,39)} = 0.339$, $P = 0.564$).

The Y-maze spontaneous alternation test was used to evaluate the short-term working memory ability of mice. The results of Y maze test were shown in Fig. 1C-D, there was no significant difference in the total arm entries among the 4 groups (Fig. 1C, 2-way ANOVA: genotype: $F_{(1,39)} = 0.468$, $P = 0.498$; treatment: $F_{(1,39)} = 0.208$, $P = 0.651$; genotype x treatment: $F_{(1,39)} = 0.159$, $P = 0.692$), suggesting that APP/PS1/tau gene mutation and SB-334867 treatment did not affect the locomotor activity of mice. However, compared with 72.6% ± 2.0% in WT+Vehicle group, the percentage of correct spontaneous alternation in 3xTg-AD+Vehicle group significantly decreased to 58.5% ± 3.7% ($P = 0.009$), and SB-334867 treatment further decreased the percentage of 3xTg-AD mice to 47.5% ± 3.6% ($P = 0.037$, Fig. 1D). Meanwhile, the percentage of correct spontaneous alternation in WT+SB-334867 group was significantly lower than that in WT+Vehicle group ($P = 0.032$). (2-way ANOVA: genotype: $F_{(1,39)} = 14.785$, $P < 0.001$; treatment: $F_{(1,39)} = 9.820$, $P = 0.003$; genotype x treatment: $F_{(1,39)} = 0.005$, $P = 0.941$). These results indicated that SB-334867 treatment further aggravated the short-term working memory impairment in 3xTg-AD mice and caused impairment in WT mice.

3.2. SB-334867 exacerbated the impairments of long-term spatial learning and memory in 3xTg-AD mice

Morris water maze test was used to evaluate the long-term spatial learning and memory ability of mice. The escape latency of mice among four groups in hidden platform test progressively decreased with the increase in training days (Fig. 2A-B, repeated measures ANOVA: day: $F_{(4,199)} = 100.468$, $P < 0.001$). On day 3–5, the average escape latency of mice in 3xTg-AD+Vehicle group was significantly longer than that in WT+Vehicle group (day 3: $P = 0.038$; day 4: $P = 0.003$; day 5: $P = 0.029$), and SB-334867 treatment further increased the average escape latency of 3xTg-AD mice (day 3: $P = 0.030$; day 4: $P = 0.006$; day 5: $P = 0.002$). Meanwhile, the mean escape latency in WT+SB-334867 group was longer than that in WT+Vehicle group on day 4 ($P = 0.029$).

The results of probe test on day 6 were shown in Fig. 2C-E. Compared with 42.2% ± 2.6% in WT+Vehicle group, the swimming time percentage in the target quadrant in 3xTg-AD+Vehicle group significantly decreased to 31.1% ± 2.2% ($P < 0.001$), and SB-334867 treatment further decreased the swimming time percentage of 3xTg-AD mice to 24.5% ± 1.9% ($P = 0.035$, Fig. 2C). Meanwhile, the number of platform crossing (Fig. 2D) in WT+Vehicle, WT+SB-334867, 3xTg-AD+Vehicle and 3xTg-AD+SB-334867 group was 3.8 ± 0.4, 3.0 ± 0.3, 2.6 ± 0.4 and 1.4 ± 0.3, respectively. Compared with WT mice, the number of platform crossing in 3xTg-AD mice was significantly reduced ($P = 0.01$), and SB-334867 treatment further reduced the number of platform crossing in 3xTg-AD mice ($P = 0.013$). In addition, the swimming time percentage in the target quadrant of WT mice significantly decreased after SB-334867 treatment ($P = 0.004$), but the number of platform crossing only showed decreased tendency without significant difference ($P = 0.125$). (2-way ANOVA: time percentage in target quadrant: genotype: $F_{(1,39)} = 20.467$, $P < 0.001$; treatment: $F_{(1,39)} = 11.903$, P=0.001; genotype x treatment: $F_{(1,39)} = 0.314$, $P = 0.578$. Platform crossing numbers: genotype: $F_{(1,39)} = 13.799$, $P < 0.001$; treatment: $F_{(1,39)} = 5.815$, P=0.021; genotype x treatment: $F_{(1,39)} = 0.344$, P=0.561).

In the visible platform test, the time to reach the platform was similar among 4 groups ($P > 0.05$, Fig. 2F), and there was no significant difference in swimming speed among 4 groups during all tests ($P > 0.05$, Fig. 2G), indicating that APP/PS1/tau gene mutation and OX1R blockade did not affect visual and motor abilities of mice. These results suggested that SB-334867 exacerbated impairments of spatial learning and reference memory in 3xTg-AD mice, and caused impairments in WT mice. The prolonged escape latency observed in hidden platform test, decreased swimming time percentage and number of platform crossing observed in probe test were the results of spatial learning and memory impairments of mice.

3.3. SB-334867 worsened the impairment of hippocampal synaptic plasticity in 3xTg-AD mice

Considering that synaptic plasticity in hippocampus is the cytological and electrophysiological basis of animal learning and memory behaviors [34], *in vivo* electrophysiological recording was performed after behavioral experiments. The input-output (I-O) curve of mice in four groups was shown in Fig. 3A. The amplitude of fEPSPs in each group of mice increased with the increase of stimulation intensity, but there was no statistically significant difference of fEPSPs amplitude under the same stimulation intensity among the four groups ($P > 0.05$). During 30 min of basal fEPSPs recording, the fEPSPs slopes of mice in each group were relatively stable and had no significant difference ($P > 0.05$, Fig. 3C-D). After paired-pulse stimulation, PPF was induced and there was no significant difference of PPF values among four groups ($P > 0.05$, Fig. 3B). These results indicated that neither APP/PS1/tau gene mutation nor SB-334867 treatment affected the basal synaptic transmission and presynaptic neurotransmitter release in mice.

After high-frequency stimulation (HFS), LTP was successfully induced in other three groups except mice in 3xTg-AD+SB-334867 group (Fig. 3C-E). At 0 min and 30 min after HFS, there was no significant difference of fEPSPs slopes between mice in WT+Vehicle group and 3xTg-AD+Vehicle group, but the fEPSPs slopes of 3xTg-AD mice at 60 min after HFS was significantly lower than that of WT mice ($P = 0.003$). (2-way ANOVA: 60 min: genotype: $F_{(1,23)} = 24.126$, $P < 0.001$; treatment: $F_{(1,23)} = 9.570$, $P = 0.006$; genotype x treatment: $F_{(1,23)} = 0.012$, $P = 0.912$). More importantly, SB-334867 treatment significantly decreased the slopes of fEPSPs in 3xTg-AD mice at 0 min ($P < 0.001$), 30 min ($P = 0.018$) and 60 min ($P = 0.035$) after HFS. Meanwhile, the slope of fEPSPs in the WT+SB-334867 group was significantly lower than that in the WT+Vehicle group at 60 min after HFS ($P = 0.048$). (2-way ANOVA: 0 min: genotype: $F_{(1,23)} = 20.913$, $P < 0.001$; treatment: $F_{(1,23)} = 22.278$, $P < 0.001$; genotype x treatment: $F_{(1,23)} = 14.226$, $P = 0.001$. 30 min: genotype: $F_{(1,23)} = 19.437$, $P < 0.001$; treatment: $F_{(1,23)} = 4.285$, $P = 0.052$; genotype x treatment: $F_{(1,23)} = 2.488$, $P = 0.130$). These results indicated that OX1R blockade by SB-334867 treatment impaired hippocampal synaptic plasticity in both 3xTg-AD mice and WT mice.

3.4. SB-334867 down-regulated the expression level of postsynaptic density 95 (PSD-95) in the hippocampus of 3xTg-AD mice

The expression levels of presynaptic SYP and postsynaptic PSD-95 in the hippocampus of mice in each group were shown in Fig. 4. Compared with WT+Vehicle group, the expression level of SYP in the hippocampus of 3xTg-AD+Vehicle group was significantly decreased ($P = 0.010$), but SB-334867 treatment did not affect SYP expression in hippocampus of both 3xTg-AD mice ($P = 0.586$) and WT mice ($P = 0.753$) (2-way ANOVA: genotype: $F_{(1,19)} = 18.553$, $P < 0.001$; treatment: $F_{(1,19)} = 0.383$, $P = 0.545$; genotype x treatment: $F_{(1,19)} = 0.028$, $P = 0.869$). At the same time, the expression level of PSD-95 in the hippocampus of mice in 3xTg-AD+Vehicle group was significantly lower than that of WT+Vehicle group ($P = 0.047$), SB-334867 treatment significantly decreased the expression levels of PSD-95 in hippocampus of both 3xTg-AD mice ($P = 0.015$) and WT mice ($P = 0.009$) (2-way ANOVA: genotype: $F_{(1,19)} = 8.216$, P=0.011; treatment: $F_{(1,19)} = 16.182$, $P < 0.001$; genotype x treatment: $F_{(1,19)} = 0.032$, $P = 0.861$). These results indicated that OX1R blockade could significantly reduce the expression of PSD-95 in hippocampus, but did not affect the expression of SYP.

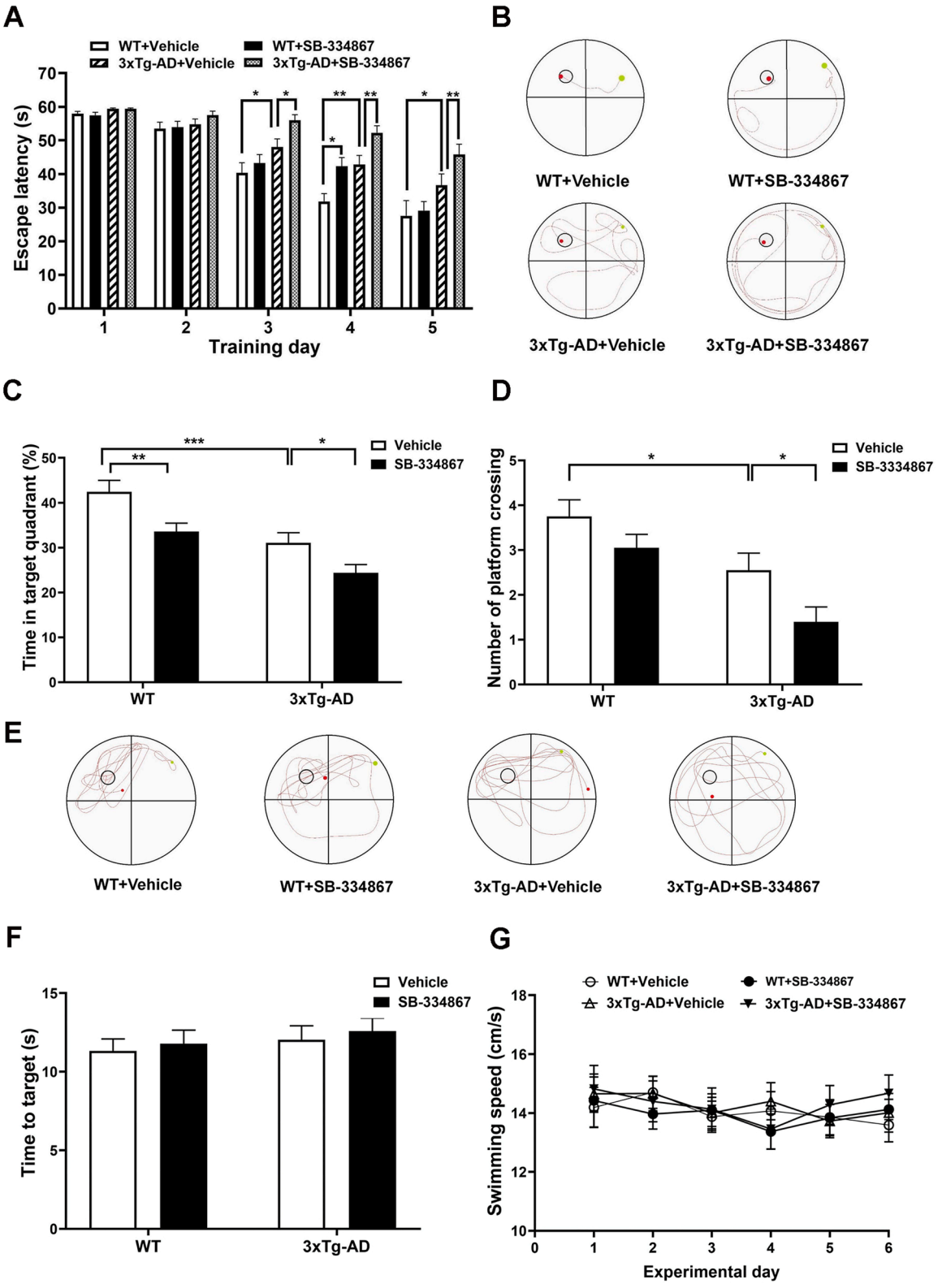

Fig. 2. SB-334867 exacerbated spatial reference memory impairment in 3xTg-AD mice. (A) Bar graphs showing the average escape latencies of mice during the 5 training days. (B) Representative swimming traces of mice on the fifth day of hidden platform test. The large circle represents the water maze pool, and the small circle represents the hidden platform. The green point was the beginning and the red point was the end of one experimental trail. (C-D) Bar graphs showing the swimming time percentage spent in target quadrant and number of platform crossing of mice in probe test. (E) Representative swimming traces of mice in probe test. (F) Bar graphs showing the average swimming time of arrival at the visible platform. (G) Line charts showing no significant difference in the average swimming speed of mice among the four groups. (n = 10, * $P < 0.05$, ** $P < 0.01$, *** $P < 0.001$).

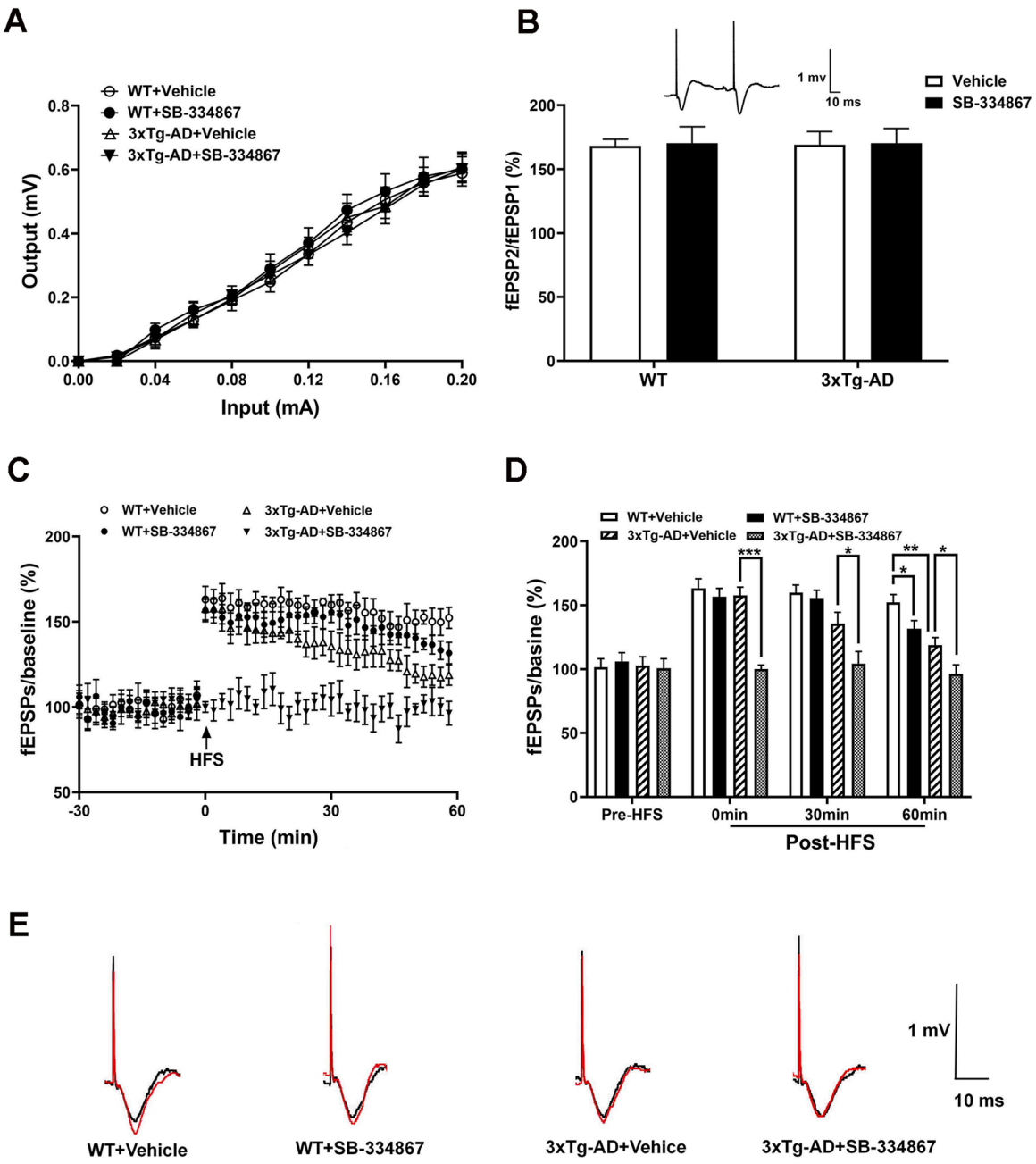

Fig. 3. SB-334867 worsened hippocampal LTP in 3xTg-AD mice. (A) Input-output curves showed no significant difference among four groups. (B) APP/PS1/tau gene mutation and SB-334867 treatment did not affect PPF among the four groups. Inset: representative trace of fEPSPs induced by paired pulse stimulation. (C) Time course of fEPSPs and LTP induced by HFS in the hippocampus of mice. (D) Bar graphs showing LTP depression in 3xTg-AD mice was aggravated by SB-334867 treatment at 0 min, 30 min and 60 min after HFS. (n = 6, * $P < 0.05$, ** $P < 0.01$, *** $P < 0.001$). (E) Typical fEPSP traces before (black) and 60 min after HFS (red) among four groups. Scale bars: 1 mV and 10 ms.

3.5. SB-334867 increased the expression levels of soluble Aβ oligomers and p-tau in the hippocampus of 3xTg-AD mice

Because Aβ oligomers played important neurotoxic role in the course of AD [2], the expression levels of Aβ oligomers in the hippocampus of 3xTg-AD mice were detected. As shown in Fig. 5A-B and Fig S1, SB-334867 treatment significantly increased the expression of Aβ oligomers ($t = 7.182$, $P < 0.001$), the levels of Aβ1–40 ($P = 0.024$) and Aβ1–42 ($P = 0.024$) in 3xTg-AD mice (2-way ANOVA: Aβ1–40: genotype: $F_{(1,15)} = 22.961$, $P < 0.001$; treatment: $F_{(1,15)} = 8.020$, $P = 0.015$; genotype x treatment: $F_{(1,15)} = 0.687$, $P = 0.423$. Aβ1–42: genotype: $F_{(1,15)} = 24.817$, $P < 0.001$; treatment: $F_{(1,15)} = 5.245$, $P = 0.041$; genotype x treatment: $F_{(1,15)} = 1.905$, $P = 0.193$).

Abnormal tau hyperphosphorylation is another important pathological characteristic of AD, which could affect the degree of dementia in AD [35]. The expression levels of phosphorylated tau (p-tau) protein and total tau (t-tau) protein in the hippocampus of mice were shown in Fig. 5C-E, the expression level of p-tau in the hippocampus of mice in 3xTg-AD+Vehicle group was significantly higher than that in WT+Vehicle group ($P = 0.008$), and SB-334867 treatment further increased the expression level of p-tau in the hippocampus of 3xTg-AD mice ($P = 0.009$) (2-way ANOVA: genotype: $F_{(1,19)} = 51.333$, $P < 0.001$; treatment: $F_{(1,19)} = 1.815$, $P = 0.197$; genotype x treatment: $F_{(1,19)} = 8.377$, $P = 0.011$).

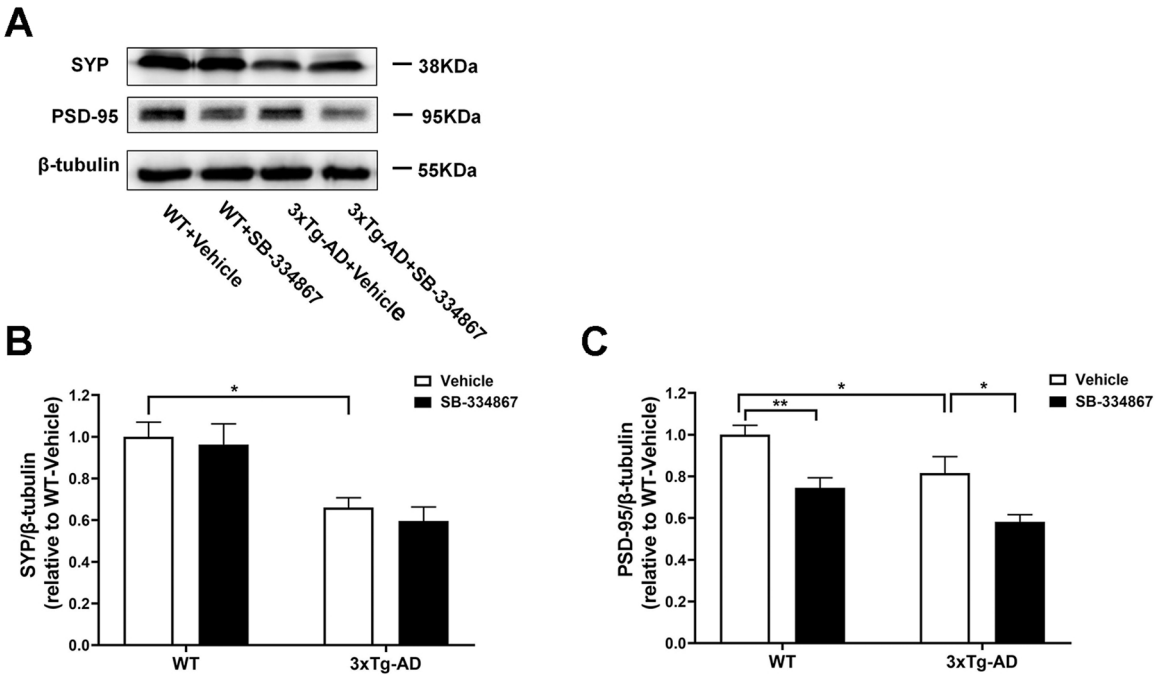

Fig. 4. SB-334867 down-regulated the expression level of PSD-95 in the hippocampus of 3xTg-AD mice. (A) Representative immunoblots of SYP and PSD-95. (B-C) Bar graphs showing the quantification of SYP and PSD-95 immunoblots density among four groups. All values were expressed as percentages of WT+Vehicle mice (n = 5, * $P < 0.05$, ** $P < 0.01$).

4. Discussion

AD is a neurodegenerative disease characterized by progressive memory loss and cognitive deficits [36]. Previous clinical evidence showed that the elevated orexin-A level in CSF was related to the abnormal levels of Aβ and tau in CSF, and the significant decrease of cognitive function in the preclinical MCI and early phase of AD patients [7,8,37]. Recent animal research showed higher density and distribution of orexin A-positive neurons in APP/PS1 mice [12], and orexin-A increased Aβ deposition, aggravated spatial reference memory impairment in APP/PS1 mice [13]. Considering that orexin exerting its effects through OX1R and OX2R [38], the expression and roles of OX1R and OX2R in AD should be investigated. Our preliminary data showed that both the expression of OX1R and OX2R increased in the hippocampus of 9-month-old 3xTg-AD mice (Fig S2). At the same time, the effects of DORA almorexant, suvorexant and DORA-22 on different AD model mice were reported before. Almorexant and suvorexant could reduce Aβ deposition, improve different types of memory impairments and alleviate *in vivo* hippocampal LTP depression in APP/PS1 mice [19,20], but DORA-22 did not affect short-term working memory and the density of amyloid plaques in 5xFAD mice [21]. Because the use of DORA could not confirm the effects of OX1R and OX2R alone in AD pathogenesis, it is important to further investigate the effects of OX1R or OX2R alone by using selective subtype antagonist. Considering that OX1R is highly expressed in the hippocampus and important to learning and memory regulation [39], the effects of OX1R on cognitive impairments in 3xTg-AD mice exhibited both Aβ and tau pathology were investigated in the present study by using OX1R antagonist SB-334867 [40,41].

Previous reports found that hippocampal injection of SB-334867 could impair memory acquisition and consolidation of rats [42]; OX1R knockdown in hippocampal CA1 region could impair spatial learning and memory in rats [17]. In the present study, SB-334867 treatment lead to impairments of object recognition, short-term working memory and long-term spatial memory of WT mice, which was similar to previous reports and testified the important roles of OX1R in cognitive function. More importantly, OX1R blockade significantly aggravated the impairments of short-term working memory and long-term spatial memory of 3xTg-AD mice, without affecting the visual acuity and motor ability. Although SB-334867 treatment further decreased the RI and DI of 3xTg-AD mice in object recognition test, it does not mean that SB-334867 further impaired the object recognition of 3xTg-AD mice because the levels of RI in both groups are lower than 50% [29,43].

Memory formation and consolidation is closely related to synaptic plasticity [44], LTP is one manifestation of increased synaptic transmission efficiency primarily involves a postsynaptic modification [45,46]. Previous research found SB-334867 could inhibit *in vivo* LTP induction in the dentate gyrus of hippocampus in rats [47], indicating the activation of OX1R was involved in the regulation of hippocampal synaptic plasticity. In the present study, SB-334867 treatment also depressed *in vivo* hippocampal LTP of WT mice, which was closely related to the decline of cognitive function observed in WT mice. However, the effects of blocking OX1R on hippocampal synaptic plasticity in 3xTg-AD mice were still unknown. So, we observed the effects of SB-334867 on basic synaptic transmission, presynaptic neurotransmitter release, and LTP of 3xTg-AD mice by using *in vivo* electrophysiological recordings after the behavioral experiments. The results showed that APP/PS1/tau gene mutation and SB-334867 treatment did not affect the basic synaptic transmission and presynaptic neurotransmitter release. However, HFS induced LTP was significantly depressed in the hippocampus of 3xTg-AD mice, and SB-334867 treatment failed to induce hippocampal LTP in 3xTg-AD mice. Therefore, the aggravation of cognitive impairments in 3xTg-AD mice after SB-334867 treatment might be the results of hippocampal synaptic plasticity depression.

SYP is the most abundant integral membrane protein in synaptic vesicles, and is involved in the regulation of synaptic development and the release of neurotransmitters [48]. PSD-95 is abundant in the brain, mainly expresses in the postsynaptic region, regulates synaptic strength by interacting with other synaptic proteins, and plays important roles in LTP induction [46,49]. Postmortem autopsy showed marked loss of SYP and PSD-95 in the hippocampus of MCI and AD patients [50–52]. In the present study, the expression levels of SYP and PSD-95 in the hippocampus of 3xTg-AD mice were obviously decreased, which was similar to previous report in the hippocampus of 9-month-old 3xTg-AD mice [53]. After SB-334867 treatment, the expression of PSD-95 in the

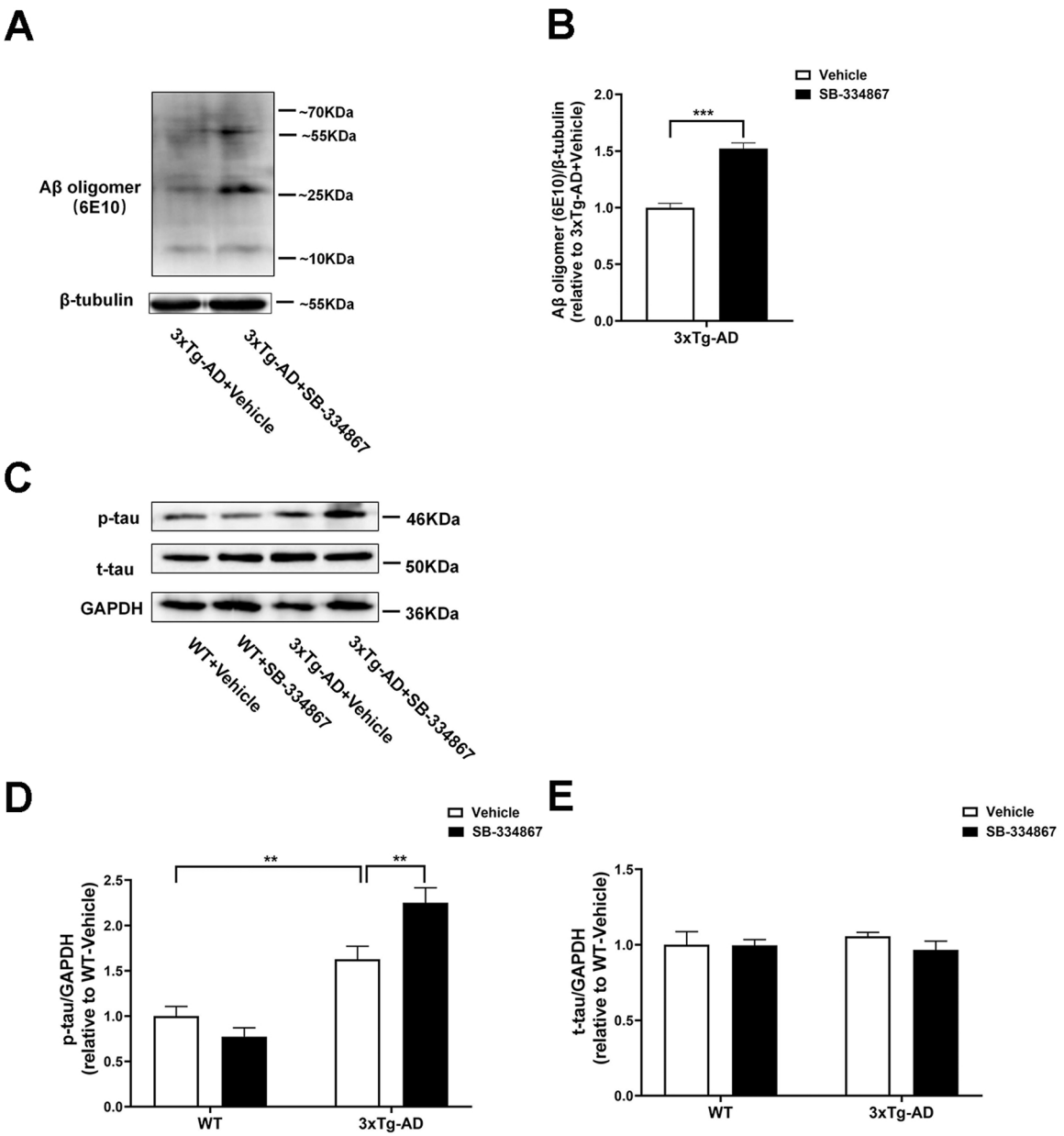

Fig. 5. SB-334867 increased the expression levels of soluble Aβ oligomers and p-tau in the hippocampus of 3xTg-AD mice (A) Representative immunoblots of soluble Aβ oligomers. (B) Bar graphs showing the quantification of soluble Aβ oligomers of 3xTg-AD mice. (n = 4, *** $P < 0.001$) (C) Representative immunoblots of p-tau and t-tau. (D-E) Bar graphs showing the quantification of p-tau and t-tau immunoblots density among four groups. All values were expressed as percentages of WT+Vehicle mice. (n = 5, ** $P < 0.01$).

hippocampus of both WT mice and 3xTg-AD mice decreased, but the expression of SYP did not change significantly. Considering that knockdown of OX1R in the hippocampus of grass rats selectively decreased mushroom spines that has the most expanded postsynaptic density [17], and phospholipase C β3 (PLCβ3) which interact with PSD-95/Dlg/ZO-1 (PDZ) domain [54] could mediate impairment of memory by long-term OX1R blockade [15], decreased PSD-95 expression observed after SB-334867 treatment might be the results of spine density reduction and PLCβ3 signaling pathway down-regulation. At the same time, these results were consistent with the electrophysiological results that SB-334867 aggravated LTP depression in 3xTg-AD mice and induced LTP depression in WT mice, but did not affect PPF values and presynaptic neurotransmitter release in two types of mice, suggesting that long-term blockade of OX1R induced the impairments of synaptic plasticity and cognitive functions in both WT and 3xTg-AD mice mainly through postsynaptic mechanism.

During the course of AD, elevated Aβ levels in the brain play pivotal roles, which could lead to hyperphosphorylation of tau protein and formation of neurofibrillary tangles, ultimately leading to neuronal death and synaptic dysfunction [55,56]. Considering that Aβ oligomers played important neurotoxic role than Aβ plaques, we detected soluble Aβ oligomers and levels of Aβ1–40 and Aβ1–42, but not Aβ plaques, in the present study. The results showed that SB-334867 significantly increased the contents of soluble Aβ oligomers and levels of Aβ1–40 and Aβ1–42 in the hippocampus of 3xTg-AD mice. Since Aβ oligomers could directly cause synaptic damage, synaptic transmission dysfunction and cognitive decline, the increased Aβ oligomers might reduce the expression of PSD-95, thereby aggravating synaptic plasticity and cognitive impairments observed in AD mice. On the other hand, pathological tau in the brain could directly exert neurotoxic effects and induce Aβ neurotoxicity [5], so the expression levels of t-tau and p-tau at Thr231 occurred at early stage in AD [57] were measured in the present study.

The results showed that SB-334867 did not affect the expression of t-tau, but significantly increased the expression of p-tau in the hippocampus of 3xTg-AD mice, which might be another important reason of SB-334867 aggravating cognitive impairment and synaptic plasticity damage in 3xTg-AD mice. However, there are different epitopes of p-tau and only one epitope detected is a weakness of present study.

As we known, the increased Aβ level in the brain is the result of disturbances in Aβ metabolism, including increased Aβ production and decreased Aβ clearance [58]. According to previous research, orexin-A could affect the phagocytosis and degradation of exogenous Aβ in microglia [59], and decrease Aβ clearance *via* the brain glymphatic system by reducing nighttime sleep [6,19,60]. Our recent research (unpublished) found that orexin-A increased the expression of β-site amyloid precursor protein cleaving enzyme 1 (BACE1) which initiates the generation of Aβ [61], decreased the expression of NEP plays an important role in Aβ degradation [58] in the hippocampus of 3xTg-AD mice. However, there is no report about how OX1R affects Aβ metabolism until now. Considering that OX1R knockout resulted in almost normal sleep-wake patterns in mice [39], the possible mechanism of OX1R blocking to affect Aβ level might not closely related to sleep-wake cycle and brain glymphatic system clearance, and SB-334867 might increase Aβ level through affecting expression levels of BCAE1 and NEP, or affecting glia cell-mediated degradation. According to the amyloid cascade hypothesis, Aβ plays pivotal roles in AD pathogenesis and can lead to hyperphosphorylation of tau protein and formation of neurofibrillary tangles [55,56,62]. The increased expression of p-tau in the hippocampus of 3xTg-AD mice after SB-334867 treatment might be the result of abnormal Aβ elevation.

In conclusion, this study indicates that long-term blockade of OX1R with SB-334867 exacerbates impairments of synaptic plasticity and cognitive function in 3xTg-AD mice. The detrimental effects of OX1R blockade in AD might be the cumulative results of both aggravating development of AD pathology and its direct damage on cognition. Meanwhile, the mechanism by which OX1R blockade increasing levels of soluble Aβ oligomers and p-tau remains to be further investigated.

CRediT authorship contribution statement

LW and MW conceived and designed the research; WG, XH, and KY performed the experiments; HC and ZW provided technical supports and data analysis; WG and MW wrote the manuscript. All authors approved the final manuscript.

Funding

This work was supported by Research Project supported by Shanxi Scholarship Council of China (No. 2020–083, 2022–115), National Natural Science Foundation of China (No. 82271484, 82171428), the Applied Basic Research Program of Shanxi Province of China (No. 20210302123306), "A batch of four" Medical Innovation Program through Science and Technology of Shanxi (No. 2021XM33).

Declaration of Competing Interest

None.

Data availability

Data will be made available on request.

Appendix A. Supporting information

Supplementary data associated with this article can be found in the online version at doi:10.1016/j.bbr.2022.114171.

References

[1] Serge Gauthier, Pedro Rosa-Neto, José A. Morais, C. Webster, World Alzheimer Report 2021 Journey through the diagnosis of dementia, (2021).
[2] M. Tolar, J. Hey, A. Power, S. Abushakra, Neurotoxic soluble amyloid oligomers drive alzheimer's pathogenesis and represent a clinically validated target for slowing disease progression, Int J. Mol. Sci. 22 (12) (2021) 6355.
[3] S.Y. Liang, Z.T. Wang, L. Tan, J.T. Yu, Tau toxicity in neurodegeneration, Mol. Neurobiol. 59 (6) (2022) 3617–3634.
[4] M.A. Busche, B.T. Hyman, Synergy between amyloid-β and tau in Alzheimer's disease, Nat. Neurosci. 23 (10) (2020) 1183–1193.
[5] A.R. Roda, G. Serra-Mir, L. Montoliu-Gaya, L. Tiessler, S. Villegas, Amyloid-beta peptide and tau protein crosstalk in Alzheimer's disease, Neural Regen. Res. 17 (8) (2022) 1666–1674.
[6] J.P. Kukkonen, P.M. Turunen, Cellular signaling mechanisms of hypocretin/orexin, Front Neurol. Neurosci. 45 (2021) 91–102.
[7] C. Liguori, M. Nuccetelli, F. Izzi, G. Sancesario, A. Romigi, A. Martorana, C. Amoroso, S. Bernardini, M.G. Marciani, N.B. Mercuri, F. Placidi, Rapid eye movement sleep disruption and sleep fragmentation are associated with increased orexin-A cerebrospinal-fluid levels in mild cognitive impairment due to Alzheimer's disease, Neurobiol. Aging 40 (2016) 120–126.
[8] C. Liguori, A. Romigi, M. Nuccetelli, S. Zannino, G. Sancesario, A. Martorana, M. Albanese, N.B. Mercuri, F. Izzi, S. Bernardini, A. Nitti, G.M. Sancesario, F. Sica, M.G. Marciani, F. Placidi, Orexinergic system dysregulation, sleep impairment, and cognitive decline in Alzheimer disease, JAMA Neurol. 71 (12) (2014) 1498–1505.
[9] C. Liguori, A. Chiaravalloti, M. Nuccetelli, F. Izzi, G. Sancesario, A. Cimini, S. Bernardini, O. Schillaci, N.B. Mercuri, P. Fabio, Hypothalamic dysfunction is related to sleep impairment and CSF biomarkers in Alzheimer's disease, J. Neurol. 264 (11) (2017) 2215–2223.
[10] W.E. Heywood, J. Hallqvist, A.J. Heslegrave, H. Zetterberg, C. Fenoglio, E. Scarpini, J.D. Rohrer, D. Galimberti, K. Mills, CSF pro-orexin and amyloid-beta38 expression in Alzheimer's disease and frontotemporal dementia, Neurobiol. Aging 72 (2018) 171–176.
[11] C. Liguori, N.B. Mercuri, M. Nuccetelli, F. Izzi, A. Cordella, S. Bernardini, F. Placidi, Obstructive sleep apnea may induce orexinergic system and cerebral beta-amyloid metabolism dysregulation: is it a further proof for Alzheimer's disease risk? Sleep. Med. 56 (2019) 171–176.
[12] P. Zhao, Y. You, Z. Wang, Y. Zhou, G. Chai, G. Yan, Z. Jin, Q. Wang, H. Sun, Orexin A peptidergic system: comparative sleep behavior, morphology and population in brains between wild type and Alzheimer's disease mice, Brain Struct. Funct. 227 (3) (2022) 1051–1065.
[13] M. Li, Y. Meng, B. Chu, Y. Shen, X. Xue, C. Song, X. Liu, M. Ding, X. Cao, P. Wang, S. Xu, J. Bi, Z. Xie, Orexin-A exacerbates Alzheimer's disease by inducing mitochondrial impairment, Neurosci. Lett. 718 (2020), 134741.
[14] S.S. Ch'ng, A.J. Lawrence, Distribution of the orexin-1 receptor (OX1R) in the mouse forebrain and rostral brainstem: a characterisation of OX1R-eGFP mice, J. Chem. Neuroanat. 66–67 (2015) 1–9.
[15] M. Kourosh-Arami, A. Komaki, M.T. Joghataei, M. Mohsenzadegan, Phospholipase Cβ3 in the hippocampus may mediate impairment of memory by long-term blockade of orexin 1 receptors assessed by the Morris water maze, Life Sci. 257 (2020), 118046.
[16] S. García-Brito, L. Aldavert-Vera, G. Huguet, E. Kádár, P. Segura-Torres, Orexin-1 receptor blockade differentially affects spatial and visual discrimination memory facilitation by intracranial self-stimulation, Neurobiol. Learn Mem. 169 (2020) 107–188.
[17] J.E. Soler, H. Xiong, F. Samad, F.P. Manfredsson, A.J. Robison, A.A. Núñez, L. Yan, Orexin (hypocretin) mediates light-dependent fluctuation of hippocampal function in a diurnal rodent, Hippocampus 31 (10) (2021) 1104–1114.
[18] D. Han, F. Han, Y. Shi, S. Zheng, L. Wen, Mechanisms of memory impairment induced by orexin-a via orexin 1 and orexin 2 receptors in post-traumatic stress disorder rats, Neuroscience 432 (2020) 126–136.
[19] J.E. Kang, M.M. Lim, R.J. Bateman, J.J. Lee, L.P. Smyth, J.R. Cirrito, N. Fujiki, S. Nishino, D.M. Holtzman, Amyloid-beta dynamics are regulated by orexin and the sleep-wake cycle, Science 326 (5955) (2009) 1005–1007.
[20] F. Zhou, X.D. Yan, C. Wang, Y.X. He, Y.Y. Li, J. Zhang, Z.J. Wang, H.Y. Cai, J.S. Qi, M.N. Wu, Suvorexant ameliorates cognitive impairments and pathology in APP/PS1 transgenic mice, Neurobiol. Aging 91 (2020) 66–75.
[21] M.J. Duncan, H. Farlow, C. Tirumalaraju, D.H. Yun, C. Wang, J.A. Howard, M. N. Sanden, B.F. O'Hara, K.J. McQuerry, A.D. Bachstetter, Effects of the dual orexin receptor antagonist DORA-22 on sleep in 5XFAD mice, Alzheimer'S. Dement. 5 (2019) 70–80.
[22] S. Oddo, A. Caccamo, J.D. Shepherd, M.P. Murphy, T.E. Golde, R. Kayed, R. Metherate, M.P. Mattson, Y. Akbari, F.M. LaFerla, Triple-transgenic model of Alzheimer's disease with plaques and tangles: intracellular Abeta and synaptic dysfunction, Neuron 39 (3) (2003) 409–421.
[23] S. Oveisgharan, Z. Arvanitakis, L. Yu, J. Farfel, J.A. Schneider, D.A. Bennett, Sex differences in Alzheimer's disease and common neuropathologies of aging, Acta Neuropathol. 136 (6) (2018) 887–900.
[24] J.T. Yang, Z.J. Wang, H.Y. Cai, L. Yuan, M.M. Hu, M.N. Wu, J.S. Qi, Sex differences in neuropathology and cognitive behavior in APP/PS1/tau triple-transgenic mouse model of Alzheimer's disease, Neurosci. Bull. 34 (5) (2018) 736–746.
[25] R. Belfiore, A. Rodin, E. Ferreira, R. Velazquez, C. Branca, A. Caccamo, S. Oddo, Temporal and regional progression of Alzheimer's disease-like pathology in 3xTg-AD mice, Aging Cell 18 (1) (2019), e12873.

[26] R. Sharf, M. Sarhan, R.J. Dileone, Orexin mediates the expression of precipitated morphine withdrawal and concurrent activation of the nucleus accumbens shell, Biol. Psychiatry 64 (3) (2008) 175–183.
[27] Z. Zhang, H.J. Wang, D.R. Wang, W.M. Qu, Z.L. Huang, Red light at intensities above 10 lx alters sleep-wake behavior in mice, Light Sci. Appl. 6 (5) (2017), e16231.
[28] M.J. Hauser, D. Isbrandt, J. Roeper, Disturbances of novel object exploration and recognition in a chronic ketamine mouse model of schizophrenia, Behav. brain Res. 332 (2017) 316–326.
[29] H. Fanet, M. Tournissac, M. Leclerc, V. Caron, C. Tremblay, S. Vancassel, F. Calon, Tetrahydrobiopterin Improves Recognition Memory in the Triple-Transgenic Mouse Model of Alzheimer's Disease, Without Altering Amyloid-beta and Tau Pathologies, J. Alzheimer'S. Dis.: JAD 79 (2) (2021) 709–727.
[30] Y. He, Y. Li, F. Zhou, J. Qi, M. Wu, Decreased circadian fluctuation in cognitive behaviors and synaptic plasticity in APP/PS1 transgenic mice, Metab. brain Dis. 35 (2) (2020) 343–352.
[31] C. Wang, W.R. Gao, J. Yin, Z.J. Wang, J.S. Qi, H.Y. Cai, M.N. Wu, Chronic sleep deprivation exacerbates cognitive and synaptic plasticity impairments in APP/PS1 transgenic mice, Behav. brain Res. 412 (2021), 113400.
[32] X.D. Yan, X.S. Qu, J. Yin, J. Qiao, J. Zhang, J.S. Qi, M.N. Wu, Adiponectin Ameliorates Cognitive Behaviors and in vivo Synaptic Plasticity Impairments in 3xTg-AD Mice, J. Alzheimer'S. Dis.: JAD 85 (1) (2022) 343–357.
[33] R.A. Nicoll, R.C. Malenka, Expression mechanisms underlying NMDA receptor-dependent long-term potentiation, Ann. N. Y. Acad. Sci. 868 (1999) 515–525.
[34] J.K. Clark, M. Furgerson, J.D. Crystal, M. Fechheimer, R. Furukawa, J.J. Wagner, Alterations in synaptic plasticity coincide with deficits in spatial working memory in presymptomatic 3xTg-AD mice, Neurobiol. Learn Mem. 125 (2015) 152–162.
[35] F. Panza, V. Solfrizzi, D. Seripa, B.P. Imbimbo, M. Lozupone, A. Santamato, C. Zecca, M.R. Barulli, A. Bellomo, A. Pilotto, A. Daniele, A. Greco, G. Logroscino, Tau-Centric Targets and Drugs in Clinical Development for the Treatment of Alzheimer's Disease, BioMed. Res. Int. 2016 (2016), 3245935.
[36] L. Guzman-Martinez, C. Calfío, G.A. Farias, C. Vilches, R. Prieto, R.B. Maccioni, New Frontiers in the Prevention, Diagnosis, and Treatment of Alzheimer's Disease, J. Alzheimer'S. Dis.: JAD 82 (s1) (2021) 51–63.
[37] A. Gabelle, I. Jaussent, C. Hirtz, J. Vialaret, S. Navucet, C. Grasselli, P. Robert, S. Lehmann, Y. Dauvilliers, Cerebrospinal fluid levels of orexin-A and histamine, and sleep profile within the Alzheimer process, Neurobiol. Aging 53 (2017) 59–66.
[38] S. Soya, T. Sakurai, Evolution of orexin neuropeptide system: structure and function, Front Neurosci. 14 (2020) 691.
[39] N.C. Dale, D. Hoyer, L.H. Jacobson, K.D.G. Pfleger, E.K.M. Johnstone, Orexin signaling: a complex, multifaceted process, Front. Cell. Neurosci. 16 (2022), 812359.
[40] A. Mohammadkhani, J.E. Fragale, C.B. Pantazis, H.E. Bowrey, M.H. James, G. Aston-Jones, Orexin-1 receptor signaling in ventral pallidum regulates motivation for the opioid remifentanil, The Journal of neuroscience: the official, J. Soc. Neurosci. 39 (49) (2019) 9831–9840.
[41] D.A. Perrey, Y. Zhang, Therapeutics development for addiction: Orexin-1 receptor antagonists, Brain Res. 1731 (2020), 145922.
[42] E. Akbari, N. Naghdi, F. Motamedi, The selective orexin 1 receptor antagonist SB-334867-A impairs acquisition and consolidation but not retrieval of spatial memory in Morris water maze, Peptides 28 (3) (2007) 650–656.
[43] M. Antunes, G. Biala, The novel object recognition memory: neurobiology, test procedure, and its modifications, Cogn. Process. 13 (2) (2012) 93–110.
[44] A. Goto, A. Bota, K. Miya, J. Wang, S. Tsukamoto, X. Jiang, D. Hirai, M. Murayama, T. Matsuda, T.J. McHugh, T. Nagai, Y. Hayashi, Stepwise synaptic plasticity events drive the early phase of memory consolidation, Science 374 (6569) (2021) 857–863.
[45] Y.D. Kulik, D.J. Watson, G. Cao, M. Kuwajima, K.M. Harris, Structural plasticity of dendritic secretory compartments during LTP-induced synaptogenesis, Elife 8 (2019), e46356.
[46] R.A. Nicoll, A. Brief, History of long-term potentiation, Neuron 93 (2) (2017) 281–290.
[47] E. Akbari, F. Motamedi, F.G. Davoodi, M. Noorbakhshnia, E. Ghanbarian, Orexin-1 receptor mediates long-term potentiation in the dentate gyrus area of freely moving rats, Behav. brain Res. 216 (1) (2011) 375–380.
[48] A.C. Kokotos, C.B. Harper, J.R.K. Marland, K.J. Smillie, M.A. Cousin, S.L. Gordon, Synaptophysin sustains presynaptic performance by preserving vesicular synaptobrevin-II levels, J. Neurochem 151 (1) (2019) 28–37.
[49] D. Vallejo, J.F. Codocedo, N.C. Inestrosa, Posttranslational modifications regulate the postsynaptic localization of PSD-95, Mol. Neurobiol. 54 (3) (2017) 1759–1776.
[50] F.J. Mirza, S. Zahid, The role of synapsins in neurological disorders, Neurosci. Bull. 34 (2) (2018) 349–358.
[51] R. Sultana, W.A. Banks, D.A. Butterfield, Decreased levels of PSD95 and two associated proteins and increased levels of BCl2 and caspase 3 in hippocampus from subjects with amnestic mild cognitive impairment: Insights into their potential roles for loss of synapses and memory, accumulation of Abeta, and neurodegeneration in a prodromal stage of Alzheimer's disease, J. Neurosci. Res 88 (3) (2010) 469–477.
[52] K.H. Gylys, J.A. Fein, F. Yang, D.J. Wiley, C.A. Miller, G.M. Cole, Synaptic changes in Alzheimer's disease: increased amyloid-beta and gliosis in surviving terminals is accompanied by decreased PSD-95 fluorescence, Am. J. Pathol. 165 (5) (2004) 1809–1817.
[53] H.Y. Cai, D. Yang, J. Qiao, J.T. Yang, Z.J. Wang, M.N. Wu, J.S. Qi, C. Hölscher, A GLP-1/GIP Dual Receptor Agonist DA4-JC Effectively Attenuates Cognitive Impairment and Pathology in the APP/PS1/Tau Model of Alzheimer's Disease, J. Alzheimer'S. Dis.: JAD 83 (2) (2021) 799–818.
[54] J.I. Hwang, H.S. Kim, J.R. Lee, E. Kim, S.H. Ryu, P.G. Suh, The interaction of phospholipase C-beta3 with Shank2 regulates mGluR-mediated calcium signal, J. Biol. Chem. 280 (13) (2005) 12467–12473.
[55] G. Paroni, P. Bisceglia, D. Seripa, Understanding the Amyloid Hypothesis in Alzheimer's Disease, J. Alzheimer'S. Dis.: JAD 68 (2) (2019) 493–510.
[56] W.S. Shin, J. Di, Q. Cao, B. Li, P.M. Seidler, K.A. Murray, G. Bitan, L. Jiang, Amyloid β-protein oligomers promote the uptake of tau fibril seeds potentiating intracellular tau aggregation, Alzheimer'S. Res. Ther. 11 (1) (2019) 86.
[57] A.F. Neves, C. Camargo, C. Premer, J.M. Hare, B.S. Baumel, M. Pinto, Intravenous administration of mesenchymal stem cells reduces Tau phosphorylation and inflammation in the 3xTg-AD mouse model of Alzheimer's disease, Exp. Neurol. 341 (2021), 113706.
[58] R. Ullah, T.J. Park, X. Huang, M.O. Kim, Abnormal amyloid beta metabolism in systemic abnormalities and Alzheimer's pathology: Insights and therapeutic approaches from periphery, Ageing Res. Rev. 71 (2021), 101451.
[59] H. An, M.H. Cho, D.H. Kim, S. Chung, S.Y. Yoon, Orexin impairs the phagocytosis and degradation of amyloid-beta fibrils by microglial cells, J. Alzheimer'S. Dis.: JAD 58 (1) (2017) 253–261.
[60] J.H. Roh, H. Jiang, M.B. Finn, F.R. Stewart, T.E. Mahan, J.R. Cirrito, A. Heda, B. J. Snider, M. Li, M. Yanagisawa, L. de Lecea, D.M. Holtzman, Potential role of orexin and sleep modulation in the pathogenesis of Alzheimer's disease, The, J. Exp. Med. 211 (13) (2014) 2487–2496.
[61] H. Hampel, R. Vassar, B. De Strooper, J. Hardy, M. Willem, N. Singh, J. Zhou, R. Yan, E. Vanmechelen, A. De Vos, R. Nistico, M. Corbo, B.P. Imbimbo, J. Streffer, I. Voytyuk, M. Timmers, A.A. Tahami Monfared, M. Irizarry, B. Albala, A. Koyama, N. Watanabe, T. Kimura, L. Yarenis, S. Lista, L. Kramer, A. Vergallo, The beta-Secretase BACE1 in Alzheimer's Disease, Biol. Psychiatry 89 (8) (2021) 745–756.
[62] J.M. Long, D.M. Holtzman, Alzheimer disease: an update on pathobiology and treatment strategies, Cell 179 (2) (2019) 312–339.